Engineering in Life Sciences

WILEY-VCH

Engineering in Life Sciences

SHORT COMMUNICATION OPEN ACCESS

Genome-Reduced *Pseudomonas putida* Outcompetes the Wild-Type Strain Upon Oxygen Depletion

Jesper W. Jensen[1] | Pablo I. Nikel[2] | John M. Woodley[1] | Helena Junicke[1]

[1]Department of Chemical and Biochemical Engineering, Technical University of Denmark (DTU), Lyngby, Denmark | [2]The Novo Nordisk Foundation Center for Biosustainability, Technical University of Denmark (DTU), Lyngby, Denmark

Correspondence: Jesper W. Jensen (jewaj@kt.dtu.dk)

Received: 9 January 2025 | **Revised:** 14 July 2025 | **Accepted:** 28 August 2025

Funding: This study was supported by the Novo Nordisk Foundation (Grant number: NNF17SA0031362).

Keywords: DO limitation | growth characteristics | genome-reduction | microbial cultivation | *Pseudomonas putida*

ABSTRACT

The broad adoption of the obligate aerobe *Pseudomonas putida* in industrial-scale production requires a good understanding of the effect of changing oxygen availability due to the dissolved oxygen (DO) gradients apparent at such a scale. To that end, both wild-type *P. putida* KT2440 and a genome-reduced derivative (strain SEM10) were subjected to different oxygen partial pressures (pO_2) in the aeration gas to evaluate the effect of low oxygen availability on growth characteristics in batch mode. Strain SEM10 consistently achieved a 12.7% higher biomass yield on glucose than the wild-type strain during non-DO limited growth, suggesting that genome reduction had no adverse effects on the overall growth properties. Furthermore, when exposed to oxygen depletion in cultivations at low pO_2 (0.0525 atm), strain SEM10 kept a similar biomass yield and maximum specific growth rate. In fact, the genome-reduced strain significantly outcompeted the wild-type strain under these conditions. SEM10 achieved 23.3% and 35.5% higher biomass yields on glucose and oxygen, respectively, compared to strain KT2440 at low pO_2. These findings indicate that the genome-reduced strain, SEM10, could endure oxygen depletion during growth and even outcompete the wild-type strain under these conditions, highlighting the advantages of using streamlined strains as a platform for industrial bioprocesses.

1 | Introduction

The obligate aerobic soil bacterium *Pseudomonas putida* has emerged as an alternative host for biochemical production over the past decades [1, 2]. The bacterium harbors a remarkable versatile metabolism that allows it to adapt readily to a range of environmental demands [3]. One particular feature of its versatile metabolism is its ability to oxidize glucose to gluconate and 2-ketogluconate through the periplasmic glucose shunt (PGS) while both generating energy and giving multiple entry points to the carbon metabolism [4, 5]. Accordingly, the versatile metabolism of *P. putida* has been the basis for the development of biochemical production of a wide range of products, from biosurfactants to biopolymers and even aromatics [6–8]. The development has not been limited to product-specific research, as the *P. putida* KT2440 strain has been subject to genome streamlining to obtain more carbon-efficient platform strains. As such, the wild-type *P. putida* KT2440 had its genome reduced by ∼4.3%, resulting in the EM383 strain, which was further reduced by ∼0.5% to yield the SEM10 strain [9–11]. For example, transposons and antibiotic resistance genes were deleted to produce strains with higher genetic stability, which are more suitable for genetic engineering. In addition, a considerable amount of prophage genes as well as the flagellar operon were deleted to reduce the metabolic burden of the genome-reduced strain [9–11]. As a result, EM383 showed improved growth characteristics such as higher maximum specific growth rate, higher biomass yield, and higher protein yields in bioreactor studies [10, 12]. Furthermore,

Summary

- An energy-efficient, genome-reduced strain of the *Pseudomonas putida* KT2440 has the potential to increase yields and rates in biochemical production.
- A lower energy consumption for futile processes, such as flagellar, allows allocation of this energy for product synthesis or survival. The latter being of importance when the strain is applied for the production of harsh biochemicals or intermediates.
- These attributes are of no use unless the obligate aerobe *P. putida* can tolerate scarce oxygen supplies that may occur in large-scale cultivations.
- Our findings suggest that the genome-reduced strain performs equally well under oxygen-limited and non-limited conditions and even outcompetes the wildtype under oxygen-limited conditions.
- This highlights, for the first time, the potential application of the genome-reduced *P. putida* strain for processes where oxygen limitation may occur.

the SEM10 strain showed similar growth profiles in shake flask cultivations compared to its predecessor [10, 11].

Cultivating microorganisms in large-scale industrial bioreactors can be challenging due to mass transfer limitations observed at that scale. The mass transfer limitations often result in gradients of, for example, substrate or dissolved oxygen (DO) [13, 14]. Such gradients expose the microorganisms to ever-changing nutrient limitations, for example, high and low DO concentrations, and may adversely affect their performance [13–15]. The effect of oxygen starvation of the wild-type *P. putida* KT2440 has previously been explored in scale-down systems, where it demonstrated a remarkable ability to endure temporal oxygen starvation [16]. Nonetheless, other studies showed that changes in oxygen availability affected biomass accumulation during growth on glycerol of *P. putida* KT2440 [17]. In addition, the different steps of PGS in *P. putida* have been reported to show different oxygen demands [5, 18].

Clearly, oxygen availability impacts the growth of *P. putida* KT2440. However, none of the studies have investigated its impact on the genome-reduced variants of *P. putida* KT2440. This study aimed to elucidate whether continued low oxygen availability affects the growth of *P. putida* KT2440 and SEM10 on glucose and whether the genome-reduced strain maintains its advantageous growth characteristics at low oxygen availability.

The *P. putida* wild-type strain, KT2440, was cultivated in shake flasks at three different agitation speeds to evaluate the effect of different oxygen transfer rates growth on glucose. The growth profiles obtained at different maximum oxygen transfer rates (OTR_{max}) (obtained by adjusting the agitation to 80, 180, and 280 rpm) are illustrated in Figures S1–S3. Changing agitation in the applied interval did not incur any apparent effect on the biomass accumulation profiles. However, the calculated maximum specific growth rates (μ_{max}) were significantly different (ANOVA, $p < 0.05$), with the lowest μ_{max} ($0.614 \pm 0.004\ h^{-1}$) observed at the highest agitation speed and the highest ($0.694 \pm 0.005\ h^{-1}$) at 180 rpm, whereas an intermediate μ, $0.664 \pm 0.017\ h^{-1}$, was observed at the lowest agitation speed. *P. putida* KT2440 appeared to be susceptible to both insufficient and excess agitation. Whereas a different *P. putida* strain, KTH2, has been shown to endure hydrodynamic stress at high agitation speeds, but reduced growth on glycerol was observed at insufficient oxygen supply [17, 19]. While the growth rate reduction at 80 rpm is caused by a lower oxygen supply, the decrease in growth rate at 280 rpm could be due to an increased oxygen supply affecting the PGS. At 280 rpm, a lower accumulation of gluconate and 2-ketogluconate (Figure S1), compared to lower agitation speeds, could be observed. Such lower accumulation of PGS intermediates was also reported for *P. putida* BM014 chemostat cultivations when the DO concentrations were high (40%–60%) compared to lower (20%), non-DO-limited conditions [18]. This suggests that higher DO concentrations might favor carbon uptake through the PGS intermediates. This may also explain the reduced growth rate, as previously reported for the gluconate and 2-ketogluconate growth phases of *P. putida* mt-2 batch cultivations [5].

Shake flask cultures are limited by the information they provide, in this case, specifically by the DO concentration. To gain insights into this aspect, the KT2440 and SEM10 strains were cultivated in batch mode using a continuously stirred tank bioreactor. The pO_2 was kept constant throughout the cultivations at either 0.21 atm (high) or 0.0525 atm (low). More specifically, a reduction of pO2 rather than agitation ensured that a low DO concentration would be present regardless of the stage of the cultivation. This approach enabled a simplified simulation of oxygen limitation at an industrial scale by maintaining constant oxygen levels, in contrast to the dynamic fluctuations commonly observed in industrial-scale bioreactors [14]. Figure 1 illustrates the growth profiles of *P. putida* KT2440 at a pO_2 of 0.21 atm and 0.0525 atm, whereas Table S1 details the biomass yields of both strains obtained from the exponential growth phase, the maximum specific growth rates can be found in Table 1. KT2440 grew as anticipated at high pO_2 (0.21 atm), with a μ_{max} of $0.596 \pm 0.007\ h^{-1}$ and a biomass yield on glucose ($Y_{X/S,exp}$) of 0.413 ± 0.011 g CDW · (g glucose)$^{-1}$. While glucose was completely depleted after approximately 9–10 h, production and consumption of both gluconate and 2-ketogluconate occurred simultaneously and prior to glucose depletion, as presented in Figure 1c. Moreover, oxygen consumption and CO_2 production followed similar trends and accumulated to the same extent. At low pO_2, KT2440 grew 7.6% more slowly ($\mu_{max} = 0.551 \pm 0.013\ h^{-1}$) but conversely reached a 10.0% higher $Y_{X/S,exp}$ ($0.454 \pm 0.017\ g \cdot g^{-1}$) during exponential growth, compared to high pO_2. In addition, the cultures grown at low pO_2 reached DO depletion after approximately 7 h, resulting in further growth reduction, as visible from the CDW concentration profiles in Figure 1b. Nonetheless, during exponential growth, KT2440 utilized oxygen more efficiently at low than at high pO_2, achieving an 11.5% higher biomass yield on O_2 ($Y_{X/O2,exp}$).

The biomass yields calculated in the exponential phase (Table S1) indicate that KT2440 utilizes glucose for growth more efficiently at low pO_2 compared to high pO_2 before oxygen is depleted. This

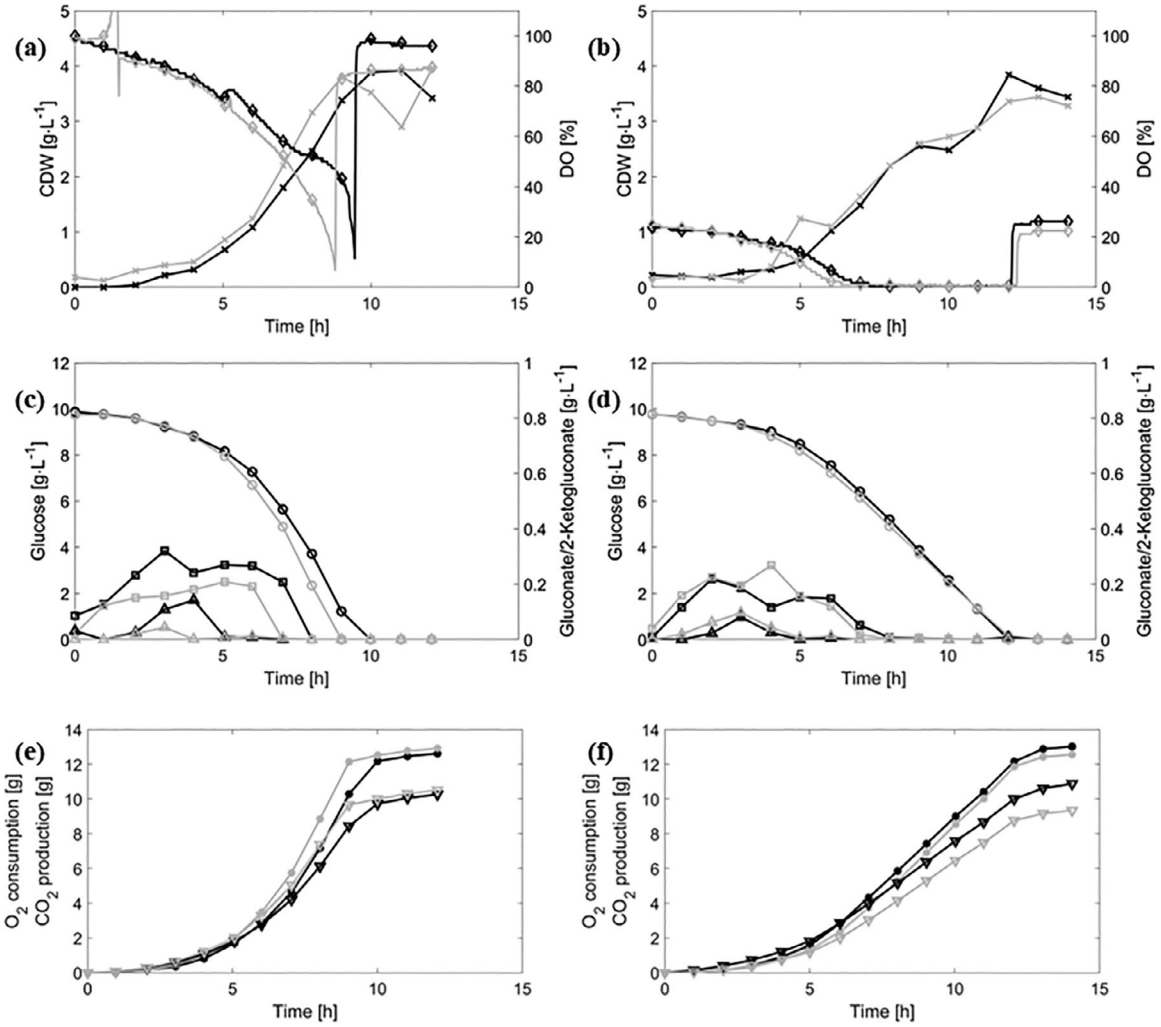

FIGURE 1 | Batch cultivation of *P. putida* KT2440 at an oxygen partial pressure of 0.21 atm ((a), (c), and (e)) and 0.0525 atm ((b), (d), and (f)). (a) and (b): CDW concentration ($g \cdot L^{-1}$, X), DO concentration (%, M). (c) and (d): Glucose concentration ($g \cdot L^{-1}$, –), gluconate concentration ($g \cdot L^{-1}$, ∀) and 2-ketogluconate concentration ($g \cdot L^{-1}$, 8). (e) and (f): consumed O_2 (g, *) and produced CO_2 (g, X). Black and light grey colors denote different replicates.

TABLE 1 | Cultivation parameters at different pO_2 for *P. putida* KT2440 and SEM10 bioreactor batch cultivations. The biomass yields and biomass concentrations were obtained at the time point of glucose depletion.

Strain	pO_2 (atm)	μ_{max} (h^{-1})	CDW_{end} ($g \cdot L^{-1}$)	$Y_{X/S, end}$ ($g \cdot g^{-1}$)	$Y_{X/O2, end}$ ($g \cdot g^{-1}$)	$Y_{X/CO2, end}$ ($g \cdot g^{-1}$)
KT2440	0.21	0.596 ± 0.007	3.94 ± 0.03	0.383 ± 0.016	0.775 ± 0.037	0.618 ± 0.031
KT2440	0.0525	0.551 ± 0.013	3.64 ± 0.28	0.352 ± 0.027	0.727 ± 0.005	0.567 ± 0.039
SEM10	0.21	0.637 ± 0.004	4.40 ± 0.25	0.432 ± 0.015	0.947 ± 0.113	0.738 ± 0.059
SEM10	0.0525	0.649 ± 0.027	4.56 ± 0.23	0.434 ± 0.008	0.985 ± 0.003	0.737 ± 0.058

contrasts with the lower final biomass concentration observed for *P. putida* KT2440 growth on glutamic acid and glycerol at reduced OTR_{max} [17, 19]. Furthermore, it contrasts the lower CDW accumulation reported for *P. putida* BM014 growth on glucose at different DO levels [18]. Considering these contrasts and the fact that the exponential growth phase only covers the non-DO limited period, yields obtained at the point of glucose depletion would better represent the entire cultivation period than yields obtained during exponential growth. Notably, KT2440 showed a similar CDW concentration of 3.64 ± 0.28 and 3.94 ± 0.03 $g \cdot L^{-1}$ at low and high pO_2, respectively, after glucose depletion. However, the biomass yields of KT2440 obtained after glucose depletion, presented in Table 1, were generally slightly lower (6%–8%) at low pO_2 compared to high pO_2.

Figure 1d showed an absence of gluconate and 2-ketogluconate after DO depletion during growth at low pO_2. This observation might indicate that glucose was phosphorylated rather than

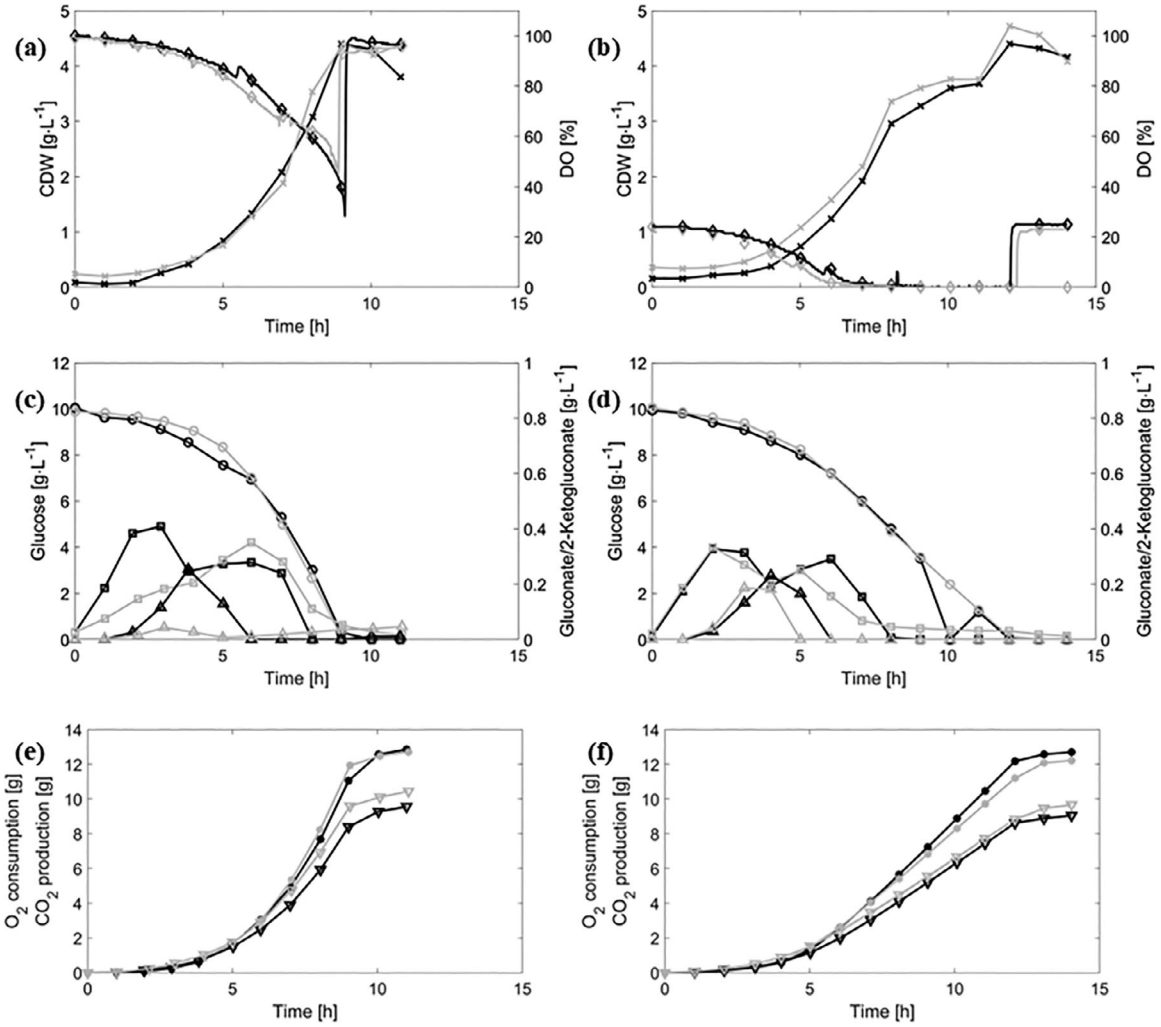

FIGURE 2 | Batch cultivation of *P. putida* SEM10 at a pO_2 of 0.21 atm ((a), (c), and (e)) and 0.0525 atm ((b), (d), and (f)). (a) and (b): CDW concentration ($g \cdot L^{-1}$, X), DO concentration (%, M). (c) and (d): Glucose concentration ($g \cdot L^{-1}$, –), gluconate concentration ($g \cdot L^{-1}$, ∀) and 2-ketogluconate concentration ($g \cdot L^{-1}$, 8). (e) and (f): consumed O_2 (g, *) and produced CO_2 (g, X). Black and light grey colors denote different replicates.

converted through the oxidative pathway in the periplasm. The absence of gluconate and 2-ketogluconate agrees with the reported lack of these metabolites during the oxygen-limited growth of *P. putida* BM014 [18]. However, Choi et al. [18] also reported a lower biomass concentration at oxygen-limited growth, which is not the case in this study. These findings suggest that *P. putida* KT2440 shifts from the conversion of glucose through the oxidative pathway to glucose conversion via phosphorylation during oxygen limitation and can retain similar biomass yields.

The genome-reduced strain, SEM10, observed the same general growth profile as KT2440 at high and low pO_2, as illustrated in Figures 1 and 2. However, as presented in Table 1, the μ_{max} was not affected by a reduction in pO_2 and remained similar across the tested conditions. The utilization of oxygen was significantly increased during exponential growth at low pO_2, which is reflected by the 19.0% increase in $Y_{X/O2,exp}$ from 0.978 ± 0.063 $g \cdot g^{-1}$ to 1.163 ± 0.018 $g \cdot g^{-1}$ at high and low pO_2, respectively. Moreover, no considerable drop in the end biomass yields presented in Table 1 was observed for SEM10 when the strain was exposed to oxygen depletion. For example, similar $Y_{X/S,end}$ of 0.432 ± 0.015 $g \cdot g^{-1}$ and 0.434 ± 0.008 $g \cdot g^{-1}$ for high and low pO_2, respectively, were obtained for the genome-reduced strain. These findings suggest that SEM10 endures the lack of sufficient oxygen supply and is, apart from the longer cultivation period, not affected by the oxygen depletion.

At high pO_2, the genome-reduced SEM10 strain grew slightly faster (6.8%) than KT2440 and achieved a 12.7% higher $Y_{X/S,end}$ (see Table 1). Correspondingly, $Y_{X/O2,end}$ and $Y_{X/CO2,end}$ at the end of the cultivation were 22.1% and 19.4% higher, respectively, compared to KT2440. Otherwise, SEM10 growth at high pO2 showed the same general trends as KT2440. Namely, the improved biomass yields of SEM10, compared to KT2440, were in good agreement with other studies comparing KT2440 and predecessors of the SEM10 strain under non-DO limited conditions [10–12]. More specifically, Lieder et al. [12] reported a 12% higher $Y_{X/S}$ for EM383 (a genome-reduced predecessor to SEM10), which is of the same magnitude as reported here. Considering that the additional deletions present in SEM10, compared to EM383, are related to genetic engineering and stability rather than

energy conservation, no increase in $Y_{X/S}$ was to be expected for SEM10 [11]. This proves that the additional genome reduction of SEM10 has not adversely affected the strain regarding growth at non-limiting DO concentrations.

While the wild-type strain observed slightly reduced biomass yields and final biomass concentrations at low pO_2 (see Table 1) compared to high pO_2, the SEM10 strain grew more efficiently and observed no considerable difference in biomass yields between the applied conditions. Notably, SEM10 accumulated 4.56 ± 0.23 $g{\cdot}L^{-1}$ CDW at low pO_2, 25.3% more than the 3.64 ± 0.28 $g{\cdot}L^{-1}$ CDW accumulated by KT2440 under similar conditions. This is further reflected in the 23.3% higher $Y_{X/S,end}$ achieved by SEM10 compared to KT2440 at low pO_2. Accordingly, these results indicate that SEM10, in regard to biomass growth, outcompetes the wild-type strain, KT2440, during oxygen depletion by retaining the previously described efficient glucose utilization.

The 26.2% lower $Y_{X/O2,max}$ of KT2440 (0.727 ± 0.005 $g{\cdot}g^{-1}$) compared to SEM10 (0.985 ± 0.003 $g{\cdot}g^{-1}$) indicates that SEM10 requires less oxygen for growth during cultivation at low pO_2. Furthermore, a similarly 23.0% lower $Y_{X/CO2,end}$ for KT2440 compared to SEM10 at low pO_2 (see Table 1) suggests that most of the consumed oxygen is used to generate ATP. This finding is supported by a 35% lower ATP maintenance requirement reported for the SEM10 predecessor, EM383, by Lieder et al. [12] under non-DO limited conditions. In general, the lower ATP maintenance requirement of EM383 should also apply to SEM10, as the latter is a further reduction of the former [11]. Lastly, low DO concentrations have been suggested elsewhere to reduce the activity of the respiratory chain of *P. putida* KT2440, thereby compromising the activity of the ATP synthase [1, 16]. Such a scenario favors SEM10 as it spends less ATP on futile cellular processes and would thus be able to allocate a scarce ATP supply more efficiently than KT2440 during DO depletion.

Genome reduction of bacterial strains does not always yield a better-performing strain or even a performance equal to the parent strain [20]. Nevertheless, the further genome reduction of SEM10 noticeably had no adverse effects on growth, as illustrated by the 12.7% increase in $Y_{X/S}$ during non-DO limited growth, which was in the same magnitude as that reported for its predecessor EM383 [12]. In addition, the SEM10 strain showed no loss in yields or growth rate during oxygen depletion, unlike the wild-type strain, which observed a modest 6%–8% reduction in biomass yields. In fact, SEM10 outcompeted KT2440 when exposed to oxygen depletion during cultivation at low pO_2, as reflected by the 23.3% and 35.5% higher $Y_{X/S,end}$ and $Y_{X/O2,end}$, respectively. This was consequently attributed to a compromised ATP generation during oxygen depletion, during which SEM10 would be able to allocate a scarce ATP supply more efficiently due to a lower ATP requirement. This attribute makes it an ideal candidate for the production of energy-demanding products, such as cis-cis muconic acid, as it may allocate scarcely available ATP more efficiently [21]. Despite the simplified simulation of oxygen limitation, these findings suggest that SEM10 can provide a platform for large-scale bioprocesses as it can withstand potential oxygen depletion at a large scale and outcompete the wild-type under such conditions.

2 | Materials and Methods

2.1 | Bacterial Strains and Medium

Bacterial strains *P. putida* KT2440 and SEM10 [11] were used in this study and stored at −80°C in 50% (w/w) glycerol. Lysogeny broth (LB) agar medium contained per liter: 10 g tryptone, 5 g yeast extract, 10 g NaCl, and 20 g agar. The defined basis medium contained per liter: 3.88 g K_2HPO_4, 2.12 g $NaH_2PO_4 \cdot 2H_2O$ and 10 mL trace element solution. The trace element solution contained per liter: 1 g EDTA, 10 g $MgCl_2 \cdot 6H_2O$, 0.2 g $ZnSO_4 \cdot 7H_2O$, 0.1 g $CaCl_2 \cdot 2H_2O$, 0.5 g $FeSO_4 \cdot 7H_2O$, 0.02 g $Na_2MoO_4 \cdot 2H_2O$, 0.02 g $CuSO_4 \cdot 5H_2O$, 0.04 g $CoCl_2 \cdot 6H_2O$ and 0.122 g $MnCl_2 \cdot 4H_2O$. Shaken cultures were supplemented with 4 and 2 $g{\cdot}L^{-1}$ $(NH_4)_2SO_4$ and bioreactor cultivations with 10 $g{\cdot}L^{-1}$ glucose and 5 $g{\cdot}L^{-1}$ $(NH_4)_2SO_4$. All chemicals were purchased from Merck (USA).

2.2 | Shake Flask Cultures

Precultures were prepared in three steps: First, glycerol stocks were activated by streaking on LB agar plates (Sarsted, Germany) and incubated at 30°C for 18 h. Second, 5 mL of a basis medium in a 14 mL cultivation tube (Falcon, Corning, Mexico), was inoculated with three colonies from a fresh LB agar plate and incubated at 30°C and 180 rpm for 8 h in a rotary shaker (Ecotron, Infors HT, Switzerland). Third, a final liquid preculture was inoculated to an initial cell dry weight (CDW) concentration of 4.59 $mg{\cdot}L^{-1}$ in 500 mL baffled shake flasks (DWK Life Sciences, United Kingdom) containing 50 mL basis medium and incubated at 30°C and 180 rpm for 18 h in a rotary shaker (Ecotron, Infors HT, Switzerland).

Shake flask cultivations were performed with 200 mL of the basis medium in 2000 mL baffled shake flasks (KAVALIERGLASS, Czech Republic). The cultures were inoculated to an initial CDW concentration of 45.9 $mg{\cdot}L^{-1}$ and incubated at 30°C and 180 rpm in a rotary shaker (Ecotron, Infors HT, Switzerland).

2.3 | Bioreactor Cultivations

Bioreactor batch cultivations were performed in a 2 L working volume EZ-control bioreactor (Getinge, Sweden). The bioreactor was inoculated with a 2% (v/v) shake flask preculture. Agitation and temperature were maintained at 1000 rpm and 30°C, respectively, throughout the cultivation. Likewise, the aeration was fixed at 2 $L_n{\cdot}min^{-1}$ with a constant pO_2 at either 0.21 atm or 0.0525 atm. The pO_2 was set by controlling individual gas flow of air and N_2 with S50 mass flow controllers (Sierra Instruments, USA). The pH was kept at 7.0 by the addition of 2 M NaOH or 2 M HCl. Antifoam agent Antifoam 204 (Sigma Aldrich, USA) was added as required aseptically with a syringe to control foaming.

2.4 | Analytics

The bioreactor off-gas composition of O_2 and CO_2 was measured online by BlueInOne Cell (BlueSens, Germany). The off-gas composition of KT2440 cultivations was measured every 16 min

and every minute for SEM10 cultivations. The KT2440 off-gas data were interpolated using a MATLAB 2019b shape-preserving piecewise cubic interpolation function to obtain data at the sampling points.

Glucose, gluconate, and 2-ketogluconate concentrations were measured by high-pressure liquid chromatography (HPLC). The analysis was performed in an Ultimate 3000 (Thermo Scientific, USA) equipped with an Aminex HPX-87H ion exchange column (Bio-Rad, USA). Operational settings were as follows: 30°C column temperature, 5 mM H_2SO_4 mobile phase, 0.6 mL·min^{-1} flow rate, detection in the refractive index and ultraviolet (UV) channel at 210 nm. Glucose and gluconate co-elute, but their concentrations were correlated by their differential contribution in the refractive index and UV channel. Samples for HPLC analysis were first filtered through a 0.2 µm cellulose acetate syringe filter (Phenomenex, USA) and then stored at −18°C prior to analysis.

Total biomass was analyzed as CDW. First, an appropriately diluted sample was filtered through a 0.2 µm polyethersulfone membrane filter (Sartorius Stedim Biotech, Germany), and secondly, the filter was flushed twice with 5 mL deionized water. Lastly, the filter was dried in a microwave oven for 20 min at 180 W and cooled for 48 h in a desiccator. The biomass content of shake flask cultivations was estimated by optical density measurements at 600 nm (OD_{600}) using a UV-1800 UV-spectrophotometer (Shimadzu, Japan). The optical density was correlated to CDW as follows:

$$CDW \quad \left(g \cdot L^{-1}\right) = 0.459 \cdot OD_{600} \tag{1}$$

2.5 | Statistical Analysis

Shake flask experiments were performed with three replicates and bioreactor experiments with two replicates. Significant differences between parameters were evaluated with either a two-tailed *t*-test or analysis of variance (ANOVA), considering p value <0.05 as significant.

Acknowledgments

This study was supported by the Novo Nordisk Fonden (Grant number: NNF17SA0031362).

Conflicts of Interest

The authors have declared no conflict of interest.

Data Availability Statement

The data that support the findings of this study are available from the corresponding author upon reasonable request.

References

1. P. I. Nikel and V. de Lorenzo, "Engineering an anaerobic Metabolic Regime in *Pseudomonas putida* KT2440 for the Anoxic Biodegradation of 1,3-dichloroprop-1-ene," *Metabolic Engineering* 15, no. 1 (2013): 98–112, https://doi.org/10.1016/j.ymben.2012.09.006.

2. I. Poblete-Castro, J. M. Borrero-de Acuña, P. I. Nikel, M. Kohlstedt, and C. Wittmann, "Host Organism: *Pseudomonas putida*," in *Industrial Biotechnology* (Wiley-VCH Verlag GmbH & Co. KGaA, 2016), 299–326, https://doi.org/10.1002/9783527807796.ch8.

3. P. I. Nikel, M. Chavarría, T. Fuhrer, U. Sauer, and V. de Lorenzo, "*Pseudomonas putida* KT2440 Strain Metabolizes Glucose Through a Cycle Formed by Enzymes of the Entner-Doudoroff, Embden-Meyerhof-Parnas, and Pentose Phosphate Pathways," *Journal of Biological Chemistry* 290, no. 43 (2015): 25920–25932, https://doi.org/10.1074/jbc.M115.687749.

4. T. del Castillo, J. L. Ramos, J. J. Rodríguez-Herva, T. Fuhrer, U. Sauer, and E. Duque, "Convergent Peripheral Pathways Catalyze Initial Glucose Catabolism in *Pseudomonas putida*: Genomic and Flux Analysis," *Journal of Bacteriology* 189, no. 14 (2007): 5142–5152, https://doi.org/10.1128/JB.00203-07.

5. L. Latrach Tlemçani, D. Corroler, D. Barillier, and R. Mosrati, "Physiological States and Energetic Adaptation During Growth of *Pseudomonas putida* mt-2 on Glucose," *Archives of Microbiology* 190, no. 2 (2008): 141–150, https://doi.org/10.1007/s00203-008-0380-8.

6. T. Hudcova, M. Halecky, E. Kozliak, M. Stiborova, and J. Paca, "Aerobic Degradation of 2,4-dinitrotoluene by Individual Bacterial Strains and Defined Mixed Population in Submerged Cultures," *Journal of Hazardous Materials* 192, no. 2 (2011): 605–613, https://doi.org/10.1016/j.jhazmat.2011.05.061.

7. I. Poblete-Castro, A. L. Rodriguez, C. M. Lam, and W. Kessler, "Improved Production of Medium-Chain-Length Polyhydroxyalkanoates in Glucose-Based Fed-Batch Cultivations of Metabolically Engineered *Pseudomonas putida* Strains," *Journal of Microbiology and Biotechnology* 24, no. 1 (2014): 59–69, https://doi.org/10.4014/jmb.1308.08052.

8. T. Tiso, N. Ihling, and S. Kubicki, et al., "Integration of Genetic and Process Engineering for Optimized Rhamnolipid Production Using *Pseudomonas putida*," *Frontiers in Bioengineering and Biotechnology* 8 (2020), https://doi.org/10.3389/fbioe.2020.00976.

9. E. Martínez-García, P. I. Nikel, T. Aparicio, and V. de Lorenzo, "Pseudomonas 2.0: Genetic Upgrading of *P. putida* KT2440 as an Enhanced Host for Heterologous Gene Expression," *Microbial Cell Factories* 13, no. 1 (2014): 1–15, https://doi.org/10.1186/s12934-014-0159-3.

10. E. Martínez-García, P. I. Nikel, M. Chavarría, and V. de Lorenzo, "The Metabolic Cost of Flagellar Motion in *Pseudomonas putida* KT2440," *Environmental Microbiology* 16, no. 1 (2014): 291–303, https://doi.org/10.1111/1462-2920.12309.

11. D. C. Volke, L. Friis, N. T. Wirth, J. Turlin, and P. I. Nikel, "Synthetic Control of Plasmid Replication Enables Target- and Self-Curing of Vectors and Expedites Genome Engineering of *Pseudomonas putida*," *Metabolic Engineering Communications* 10 (2020): e00126, https://doi.org/10.1016/j.mec.2020.e00126.

12. S. Lieder, P. I. Nikel, V. de Lorenzo, and R. Takors, "Genome Reduction Boosts Heterologous Gene Expression in *Pseudomonas putida*," *Microbial Cell Factories* 14, no. 23 (2015): 1–14, https://doi.org/10.1186/s12934-015-0207-7.

13. M. Kuschel and R. Takors, "Simulated Oxygen and Glucose Gradients as a Prerequisite for Predicting Industrial Scale Performance a Priori," *Biotechnology and Bioengineering* 117, no. 9 (2020): 2760–2770, https://doi.org/10.1002/bit.27457.

14. G. Nadal-Rey, D. D. McClure, J. M. Kavanagh, et al., "Development of Dynamic Compartment Models for Industrial Aerobic Fed-Batch Fermentation Processes," *Chemical Engineering Journal* 420, no. 3 (2021), https://doi.org/10.1016/j.cej.2021.130402.

15. M. Kuschel, F. Siebler, and R. Takors, "Lagrangian Trajectories to Predict the Formation of Population Heterogeneity in Large-Scale Bioreactors," *Bioengineering* 4, no. 4 (2017): 27, https://doi.org/10.3390/bioengineering4020027.

16. P. Demling, A. Ankenbauer, B. Klein, et al., "*Pseudomonas putida* KT2440 Endures Temporary Oxygen Limitations," *Biotechnology and Bioengineering* 118, no. 12 (2021): 4735–4750, https://doi.org/10.1002/bit.27938.

17. A. Rodriguez, S. Escobar, E. Gomez, V. E. Santos, and F. Garcia-Ochoa, "Behavior of Several *Pseudomonas putida* Strains Growth Under Different Agitation and Oxygen Supply Conditions," *Biotechnology Progress* 34, no. 4 (2018): 900–909, https://doi.org/10.1002/btpr.2634.

18. W. J. Choi, E. Y. Lee, and C. Y. Choi, "Effect of Dissolved Oxygen Concentration on the Metabolism of Glucose in *Pseudomonas putida* BM014," *Biotechnology and Bioprocess Engineering* 3, no. 2 (1998): 109–111, https://doi.org/10.1007/BF02932512.

19. S. Escobar, A. Rodriguez, E. Gomez, A. Alcon, V. E. Santos, and F. Garcia-Ochoa, "Influence of Oxygen Transfer on *Pseudomonas putida* Effects on Growth Rate and Biodesulfurization Capacity," *Bioprocess and Biosystems Engineering* 39, no. 4 (2016): 545–554, https://doi.org/10.1007/s00449-016-1536-6.

20. M. Ziegler and R. Takors, "Reduced and Minimal Cell Factories in Bioprocesses: Towards a Streamlined Chassis," in *Minimal Cells: Design, Construction, Biotechnological Applications* (Springer International Publishing, 2020), 1–44, https://doi.org/10.1007/978-3-030-31897-0_1.

21. M. Kohlstedt, S. Starck, N. Barton, et al., "From Lignin to Nylon: Cascaded Chemical and Biochemical Conversion Using Metabolically Engineered *Pseudomonas putida*," *Metabolic Engineering* 47 (2018): 279–293, https://doi.org/10.1016/j.ymben.2018.03.003.

Supporting Information

Additional supporting information can be found online in the Supporting Information section.

Supporting file 1: elsc70046-sup-0001-SuppMat.docx